Proceedings of Symposium on Advances of Mechanics
In Honor of President Robert R. Hwang
May 12, 2006, Keelung, Taiwan

Recent development of the null-field integral equation approach for engineering problems with circular boundaries

J. T. Chen

Distinguished Professor, Department of Harbor and River Engineering, National Taiwan Ocean University, Keelung 20224, Taiwan

E-mail: jtchen@mail.ntou.edu.tw

Summary

In this paper, a systematic approach is proposed to deal with engineering problems containing circular boundaries. The mathematical tools, degenerate kernels and Fourier series, are utilized in the null-field integral formulation. The kernel function is expanded to the degenerate form and the boundary density is expressed in terms of Fourier series. By moving the null-field point to the boundary, the singularity is novelly eliminated. Three gains of singularity free, boundary-layer effect free and exponential convergence are achieved. By matching the boundary condition, a linear algebraic system is obtained. After obtaining the unknown Fourier coefficients, the solution can be obtained by using the integral representation. This systematic approach can be applied to solve the Laplace, Helmholtz, biharmonic and biHelmholtz problems. Besides, the circular inclusion as well as the electro-mechanical coupling of piezoelectricity are addressed. Finally, several examples, including Stokes flow and piezoelectricity, are demonstrated to show the validity of present formulation.

Introduction

Engineering problems with circular holes are often encountered, e.g, missiles, aircraft, naval architecture, etc., either to reduce the weight of the whole structure or to increase the range of inspection as well as piping purposes. Analytical approach using bi-polar coordinate [1] was developed for two-holes problems. Complex variable techniques were also employed for the annular case. For a problem with several holes, many numerical methods, e.g. finite element method (FEM) and boundary element method (BEM), were resorted to solve. To develop a systematic approach for engineering problems with circular boundaries is not trivial.

Null field integral equation approach is used widely for obtaining the numerical solutions to engineering problems. Various names, e.g, T-matrix method [2] and extended boundary condition method (EBCM) [3] have been coined. A crucial advantage of this method consists in the fact that the influence matrix can be computed easily. Although many works for acoustic and water wave problems have been done, we focus on the solid mechanics here.

In this paper, we review the recent development of the null-field integral equation approach [4-10] for boundary value problems (BVPs) with circular boundaries. The key idea is the expansion of kernel functions and boundary densities in the null-field integral equations. Vector decomposition technique using the adaptive observer system is required for nonfocal cases. Applications to the Laplace, Helmholtz, biHelmholtz and biharmonic problems are addressed. Not only interior problems but also exterior cases are solved. Emphases on the inclusion as well as piezoelectricity studies are done. Several examples were demonstrated to see the validity of the new formulation.

Null-field integral equation approach for boundary value problems

Suppose there are N randomly distributed circular cavities bounded in the domain D and enclosed with the boundary, B_k ($k = 0, 1, 2, \cdots, N$) as shown in Fig. 1. We define

$$B = \bigcup_{k=0}^{N} B_k \,. \tag{1}$$

In mathematical physics, boundary value problems can be modelled by the governing equation,

$$\mathcal{L}\, u(\mathrm{x}) = 0\,,\ \mathrm{x} \in D\,, \tag{2}$$

where $\mathcal{L}$ may be the Laplace, Helmholtz, biHelmholtz or biharmonic operator, $u(\mathrm{x})$ is the potential function and D is the domain of interest. The integral equation for the domain point can be derived from the third Green's identity or Rayleigh Green identity, we have

$$2\pi u(\mathrm{x}) = \int_B T(\mathrm{s},\mathrm{x})u(\mathrm{s})dB(\mathrm{s}) - \int_B U(\mathrm{s},\mathrm{x})t(\mathrm{s})dB(\mathrm{s}),\ \mathrm{x} \in D, \tag{3}$$

$$2\pi \frac{\partial u(\mathrm{x})}{\partial \mathbf{n}_{\mathrm{x}}} = \int_B M(\mathrm{s},\mathrm{x})u(\mathrm{s})dB(\mathrm{s}) - \int_B L(\mathrm{s},\mathrm{x})t(\mathrm{s})dB(\mathrm{s}),\ \mathrm{x} \in D, \tag{4}$$

where s and x are the source and field points, respectively, B is the boundary, $\mathbf{n}_{\mathrm{x}}$ denotes the outward normal vector at the field point x and the kernel function $U(\mathrm{s},\mathrm{x})$, is the fundamental solution, and the other kernel functions, $T(\mathrm{s},\mathrm{x})$, $L(\mathrm{s},\mathrm{x})$ and $M(\mathrm{s},\mathrm{x})$, are defined in the dual boundary integral method (BIEM) [10]. It is noted that more potentials are needed in Eqs. (3) and (4) for biharmonic and biHelmholtz cases [6, 19].

By moving the field point to the boundary, the Eqs. (3) and (4) reduce to

$$\pi u(\mathrm{x}) = C.P.V.\int_B T(\mathrm{s},\mathrm{x})u(\mathrm{s})dB(\mathrm{s}) - R.P.V.\int_B U(\mathrm{s},\mathrm{x})t(\mathrm{s})dB(\mathrm{s}),\ \mathrm{x} \in B, \tag{5}$$

$$\pi \frac{\partial u(\mathrm{x})}{\partial \mathbf{n}_{\mathrm{x}}} = H.P.V.\int_B M(\mathrm{s},\mathrm{x})u(\mathrm{s})dB(\mathrm{s}) - C.P.V.\int_B L(\mathrm{s},\mathrm{x})t(\mathrm{s})dB(\mathrm{s}),\ \mathrm{x} \in B, \tag{6}$$

where *C.P.V.*, *R.P.V.* and *H.P.V.* denote the Cauchy principal value, Riemann principal value and Hadamard principal value, respectively. Once the field point x locates outside the domain, the null-field integral equations yield

$$0 = \int_B T(\mathrm{s},\mathrm{x})u(\mathrm{s})dB(\mathrm{s}) - \int_B U(\mathrm{s},\mathrm{x})t(\mathrm{s})dB(\mathrm{s}),\ \mathrm{x} \in D^c, \tag{7}$$

$$0 = \int_B M(\mathrm{s},\mathrm{x})u(\mathrm{s})dB(\mathrm{s}) - \int_B L(\mathrm{s},\mathrm{x})t(\mathrm{s})dB(\mathrm{s}),\ \mathrm{x} \in D^c, \tag{8}$$

where D^c is the complementary domain. For the circular-inclusion problem, multi-domain approach by taking the free body of each inclusion should be introduced. The continuity of displacement and equilibrium of traction should be considered on the interface between the matrix and inclusions [8,9].

Expansions of the fundamental solution and boundary density

Instead of directly calculating the CPV and HPV in Eqs.(5) and (6), we obtain the linear algebraic system from the null-field integral equations of (7) and (8) through the kernel expansion.

Based on the separable property, the kernel function $U(\mathrm{s},\mathrm{x})$ can be expanded into the separable form by dividing the source and field point in the polar coordinate:

$$U(\mathrm{s},\mathrm{x}) = \begin{cases} U^i(\mathrm{s},\mathrm{x}) = A(\mathrm{s})B(\mathrm{x}), & |\mathrm{s}| \geq |\mathrm{x}|, \\ U^e(\mathrm{s},\mathrm{x}) = A(\mathrm{x})B(\mathrm{s}), & |\mathrm{x}| \geq |\mathrm{s}|, \end{cases} \tag{9}$$

where the $A(\mathrm{x})$ and $B(\mathrm{x})$ can be found for the Laplace [4,7,8,9], Helmholtz [5], biharmonic [6] and biHelmholtz [19] operators and the superscripts "i" and "e" denote the interior ($|\mathrm{s}| > |\mathrm{x}|$) and exterior ($|\mathrm{x}| > |\mathrm{s}|$) cases, respectively. To classify the interior and exterior regions, Fig. 2 shows for one, two and three dimensional cases. For the degenerate form of

T, L and M kernels, they can be derived according to their definitions.

We apply the Fourier series expansions to approximate the potential u and its normal derivative t on the circular boundary

$$u(\mathrm{s}_k) = a_0^k + \sum_{n=1}^{m} (a_n^k \cos n\theta_k + b_n^k \sin n\theta_k) \quad , \mathrm{s}_k \in B_k, k = 0, 1, 2, \cdots, N, \tag{10}$$

$$t(\mathrm{s}_k) = p_0^k + \sum_{n=1}^{m} (p_n^k \cos n\theta_k + q_n^k \sin n\theta_k) \quad , \mathrm{s}_k \in B_k, k = 0, 1, 2, \cdots, N, \tag{11}$$

where a_n^k, b_n^k, p_n^k and q_n^k ($n = 0, 1, 2, \cdots$) are the Fourier coefficients and θ_k is the polar angle measured with respect to the x-direction.

After collocating points in the null-field integral equation of Eq. (7), the boundary integrals through all the circular contours are required. The observer system is adaptively to locate the origin at the center of circle in the boundary integrals. Adaptive observer system is chosen to fully employ the property of degenerate kernels. Figure 1 shows the boundary integration for the circular boundaries in the adaptive observer system. It is worth noting that the origin of the observer system is located on the center of the corresponding circle under integration to entirely utilize the geometry of circular boundary for the expansion of degenerate kernels and boundary densities.

By collocating the null-field point x_k on the *kth* circular boundary for Eq. (7) in Fig. 1, we have

$$0 = \sum_{k=0}^{N} \int_{B_k} T(\mathrm{s}_k, \mathrm{x}_j) u_k(\mathrm{s}) dB_k(\mathrm{s}) - \sum_{k=0}^{N} \int_{B_k} U(\mathrm{s}_k, \mathrm{x}_j) t_k(\mathrm{s}) dB_k(\mathrm{s}), \ \mathrm{x} \in D^c, \tag{12}$$

where N is the number of circles including the outer boundary and the inner circular holes. Therefore, a linear algebraic system is obtained

$$[\mathbf{U}]\{\mathbf{t}\} = [\mathbf{T}]\{\mathbf{u}\}, \tag{13}$$

where $[\mathbf{U}]$ and $[\mathbf{T}]$ are the influence matrices with a dimension of $(N+1)(2m+1)$ by $(N+1)(2m+1)$, $\{\mathbf{u}\}$ and $\{\mathbf{t}\}$ denote the column vectors of Fourier coefficients with a dimension of $(N+1)(2m+1)$ by 1 in which m indicates the truncated terms of Fourier series. After the boundary unknowns are solved by using Eq. (13), the field potential can be easily obtained according to Eq. (3).

Illustrative examples

Case 1: Infinite medium with two circular holes under the anti-plane shear (Laplace equation)

A hole centered at the origin of radius a_1 and the other hole of radius $a_2 = 2a_1$ centered on x axis at $a_1 + a_2 + d$ are shown in Fig. 3. In order to be compared with the Honein et al.'s results [11] obtained by using the Möbius transformation, the stress along the boundary of radius a_1 is shown in Fig. 3 and good agreement is made.

Case 2: A circular bar with three circular holes under torsion (Laplace equation)

A circular bar with three equal circular holes removed is under torque at the end [12,13]. The contour plot of the axial displacement is shown in Fig. 4. Good agreement is made after comparing with the Caulk's data [13] .

Case 3: A circular beam with two circular holes under bending (Laplace equation)

Consider a circular beam with two circular holes under bending [14]. One of the holes is concentric, and the other lies on the x axis. The stress concentration for $D/d = 0.0625$ (D is the distance between the two holes) is shown in Fig. 5. Our numerical results are well compared with the Bird and Steele's data [15].

Case 4: Infinite medium with three circular inclusions under the anti-plane shear (Laplace equation)

Figure 6 shows that three identical inclusions subjected to the uniform shear stress $\sigma_{zy}^{\infty} = \tau_{\infty}$ at infinity. The three inclusions form an equilateral triangle and are placed at a distance $d = 4a_1$ apart. We evaluate the hoop stress $\sigma_{z\theta}$ in the matrix around the boundary of the inclusion located at the origin as shown in Fig. 6. Good agreement is obtained between

the Gong's results [16] and ours. It is obvious that the limiting case of circular holes ($\mu_1/\mu_0 = \mu_2/\mu_0 = \mu_3/\mu_0 = 0.0$) leads to the maximum stress concentration at $\theta = 0^\circ$, which is larger than 2 of a single hole due to the interaction effect.

Case 5: Piezoelectric problem with two circular inclusions under the anti-plane shear and in-plane electric field (Laplace equation)

As the two circular inclusions are arrayed perpendicular to the coupled loadings of electrics and mechanics, the contour of shear stress σ_{zy} are plotted in Figs.7. The contour of shear stress matches very well with the Wang and Shen's results [17].

Case 6: Eigensolution for an eccentric membrane (Helmholtz equation)

An eccentric case with radii a_1 and a_2 ($a_1 = 0.5, a_2 = 2.0$) is considered as shown in Fig. 8. The boundary condition is subject to the Dirichlet type. The result matches well with those of FEM and BEM [18] as shown in Fig. 8.

Case 7: Eigensolution for an eccentric plate (biHelmholtz equation)

An eccentric plate with radii a_1 and a_2 ($a_1 = 0.25, a_2 = 1.0$) is considered as shown in Fig. 9. The plate is fixed on the outer boundary and free inside. The result matches well with those of FEM and BEM [19] as shown in Fig. 9.

Case 8: Five scatters of cylinders (Helmholtz equation-exterior acoustics).

Plane wave scattering by five soft circular cylinders is solved by using the present method. The real-part solution in Fig.10 agrees well with that of multiple DtN method [20].

Case 9: A semi-cylindrical alluvial valley for the incident SH-wave (Helmholtz equation - half plane problem)

A semi-cylindrical alluvial valley for the incident SH-wave is considered. Figure 11 shows the surface displacement for vertical incidence ($\gamma = 0^\circ$) of SH-wave versus the dimensionless frequency η. Agreement with the Trifunac's result [21] is obtained.

Case 10: Stokes' problem (biharmonic equation)

An eccentric case of Stokes' flow problem is considered. The inner cylinder is rotating with a constant angular velocity and the outer one is stationary. The stream function is shown in Fig. 12 and matches well with that of BEM [22,23].

Conclusions

A semi-analytical approach was proposed for solving BVPs with circular boundaries. Some recent results were reviewed. Although the BIE for the boundary point was employed, we need not to face the problems of CPV and HPV after introducing the degenerate kernel. Not only the singularity is transformed to the series sum but also the boundary-layer effect is eliminated. In order to verify the formulation, applications to the Laplace, Helmholtz, biharmonic and biHelmholtz problems were done. Extension to other shapes, e.g. ellipse, as well as three dimensional problems is straightforward once the degenerate kernel is available.

Acknowledgement

The financial support from NSC project with Grants no. NSC 94-2211-E-019-009 as well as the numerical results implemented by the author's students, Mr. Wen-Cheng Shen, Mr. Chai-Tsung Chen, Mr. Chia-Chun Hsiao, Mr. An-Chien Wu, Mr. Po-Yuan Chen, Mr. Ying-Te Lee and the cooperator Dr. Wei-Ming Lee are highly appreciated.

References

1. Lebedev N.N., Skalskaya I. P. and Uyand Y. S. (1979) "Worked problem in applied methematics", *Dover Publications*, New York.
2. Watermann, P. C. (1965) Matrix formulation of electromagnetic scattering, *Proc. IEEE* Vol.53, pp.805-812.
3. Doicu A. and Wriedt T. (1997) Extended boundary condition method with multiple sources located in the complex plane, Optics Commun., Vol.139 , PP.85-91.
4. Chen, J. T., Shen, W. C. and Wu, A. C. (2005) "Null-field integral equations for stress field

around circular holes under anti-plane shear", *Engineering Analysis with Boundary Elements*, Vol. 30, pp. 205-217.

5. Chen, C. T. (2005) "Null-field integral equation approach for Helmholtz (interior and exterior acoustic) problem with circular boundaries", Master Thesis, Department of Harbor and River Engineering, National Taiwan Ocean University, Taiwan.
6. Chen, J. T., Hsiao, C. C. and Leu, S. Y. (2006) Null-field integral equation approach for plate problems with circular holes, *ASME J. Appl. Mech.*, Vol.73, July (to Appear)
7. Chen J. T., Shen W. C. and Chen P. Y. (2006) Analysis of circular torsion bar with circular holes using null-field approach, *Computer Modelling in Engineering Science*, Vol.12, No.2, pp.109-119.
8. Chen J. T. and Wu A. C. (2006) Null-field integral equation approach for multi-inclusion problem under anti-plane shear, *ASME J. Appl. Mech.*, Accepted.
9. Chen J.T. and Wu A. C. (2006) Null-field integral equation approach for piezoelectricity problems with arbitrary circular inclusions, *Engineering Analysis with Boundary Elements*, Accepted.
10. Chen J. T. (2005) Null filed integral equation approach for boundary vale problems with circular boundaries, Keynote lecture of ICCES 2005, India.
11. Honein E, Honein T, Herrmann G. (1992) "On two circular inclusions in harmonic problems" *Quarterly of Applied Mathematics*, Vol. 50, pp. 479-499.
12. Ling C. B. (1947): "Torsion of a circular tube with longitudinal circular holes", *Quarterly of Applied Mathematics*, **5**, 168-181.
13. Caulk D. A. (1983) "Analysis of elastic torsion in a bar with circular holes by a special boundary integral method", *ASME Journal of Applied Mechanics*, 50, 101-108.
14. Naghdi, A. K. (1991) Bending of a Perforated Circular Cylindrical Cantilever. *International Journal of Solids and Structures*. Vol. 28 (6), pp. 739-749.
15. Bird, M. D., Steele, C. R. (1992) A Solution Procedure for Laplace's Equation on Multiply Connected Circular Domains. *ASME Journal of Applied Mechanics*, Vol. 59, pp. 398-404.
16. Gong, S. X. (1995) "Antiplane interaction among multiple circular inclusions, *Mechanics Research Communications*," **22**(3), pp.257-262.
17. Wang X., Shen Y.P. (2001) On double circular inclusion problem in antiplane piezoelectricity. *International Journal of Solids and Structures* Vol.**38**: 4439-4461.
18. Chen J. T., Lin J. H., Kuo S. R. and Chyuan, S. W. (2001) "Boundary element analysis for the Helmholtz eigenvalue problems with a multiply connected domain", *Proc. R. Soc. Lond. A*, Vol. 457, pp.2521-2546.
19. Lee W. M., Chen J. T. and Lee Y. T. (2006) Free vibration analysis of circular plates with multiple circular holes using indirect BEMs, 第十四屆振動噪音研討會,宜蘭市.
20. Grote M. J. and Kirsch C. (2004) "Dirichlet to Neumann boundary conditions for multiple scattering problems", *J. Comp. Physics*, Vol. 201, pp. 630-650.
21. Trifunac, M. D. (1971) "Surface motion of a semi-cylindrical alluvial valley for incident plane SH waves", *Bulletin the Seismological Society of America*, 61(6), pp.1755-1770.
22. Kelmanson, M. A. (1983) Boundary integral equation analysis of singular, potential and biharmonic problems, Ph.D. Thesis, Department of Applied Mathematics, University of Leeds.
23. Ingham, D. B. and Kelmanson, M. A. (1984) "Boundary Integral Equation Analyses of Singular, Potential, and Biharmonic Problems", *Lecture notes in engineering*; Vol. 7, Springer-Verlag Berlin, Heidelberg.

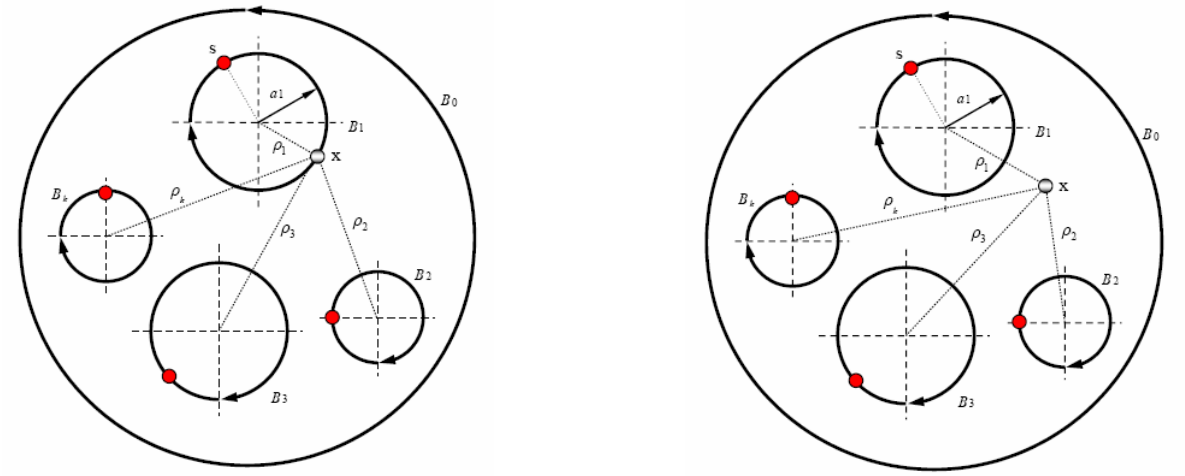

Fig. 1. Sketch of null-field and domain points in conjunction with the adaptive observer system (left: boundary point, right: null-field point).

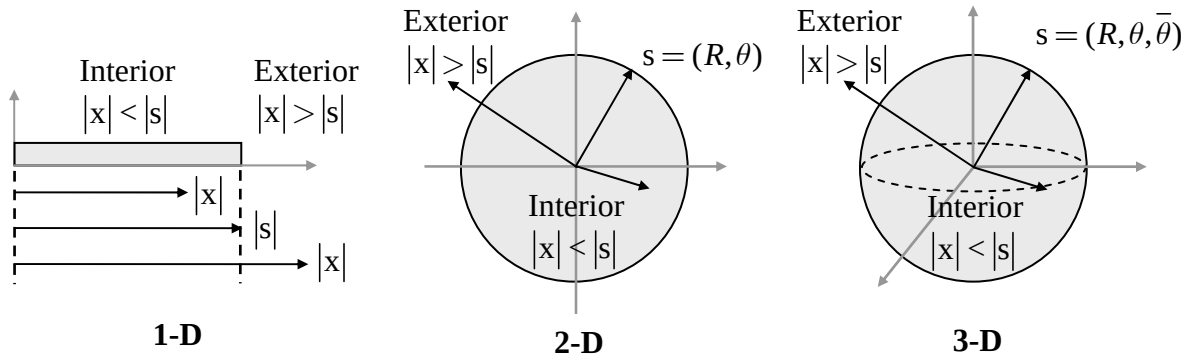

Fig. 2. The degenerate kernel for the one, two and three dimensional problems.

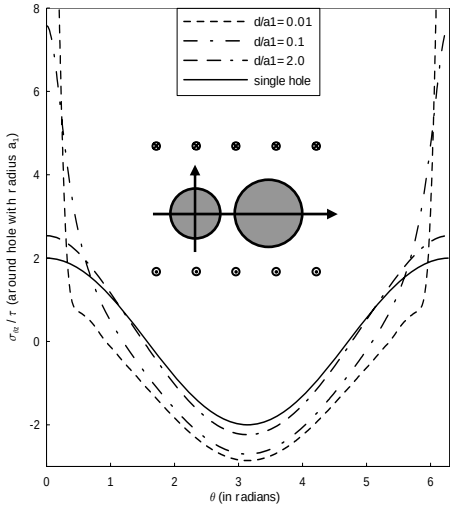

Fig. 3. Stress around the hole of radius a_1. **(Laplace equation)**

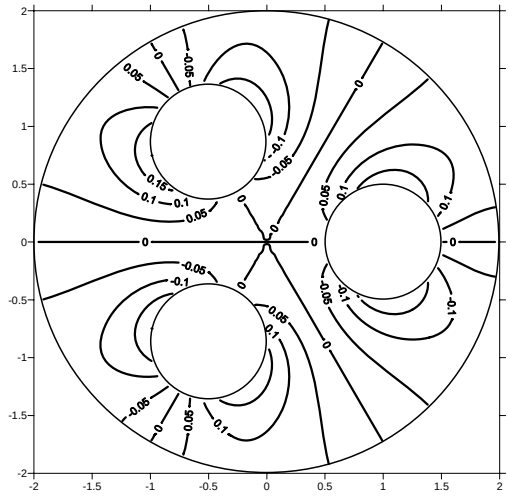

Fig. 4. Displacement for the circular bar weakened by three holes. **(Laplace equation)**

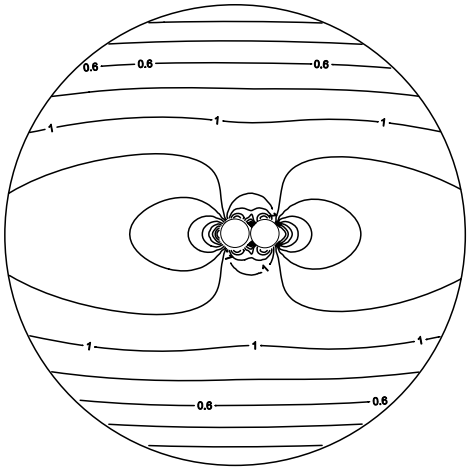

Fig. 5. Contour of stress concentration for $D/d = 0.0625$. **(Laplace equation)**

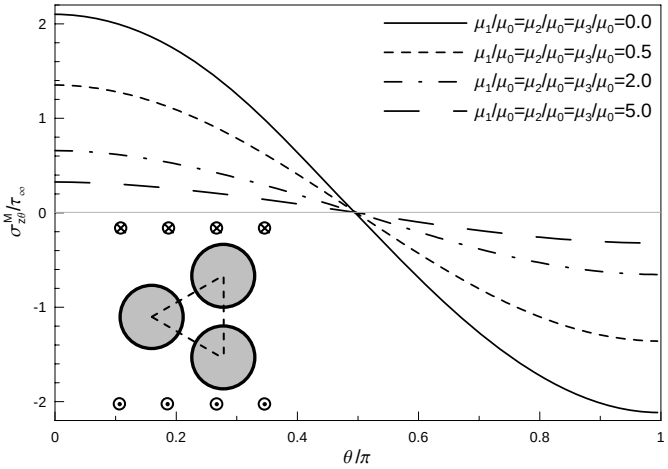

Fig. 6. Tangential stress distribution around the inclusion located at the origin. **(Laplace equation)**

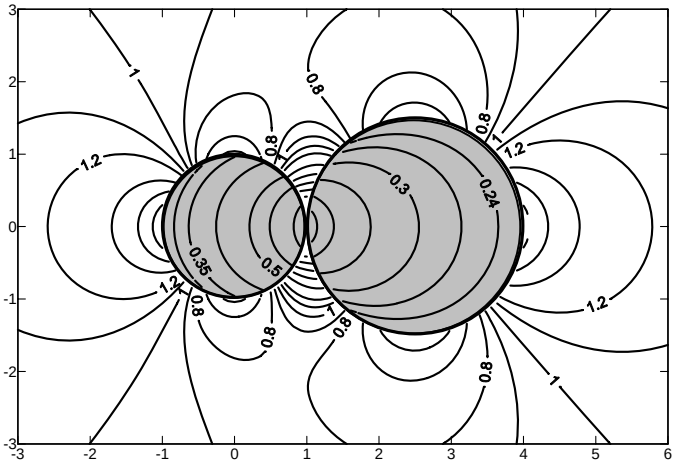

Fig. 7. Contour of shear stress σ_{zy}/τ_∞. **(Laplace equation)**

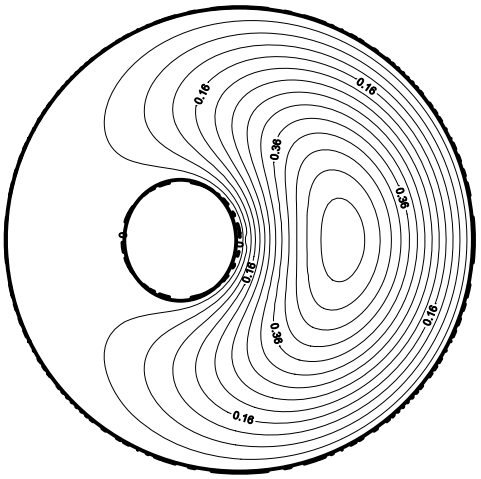

Fig. 8. The first mode of eccentric membrane. **(Helmholtz equation)**

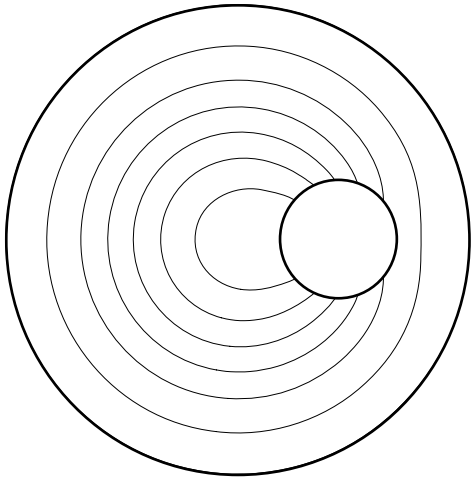

Fig. 9. The first mode of eccentric plate.
(biHelmholtz equation)

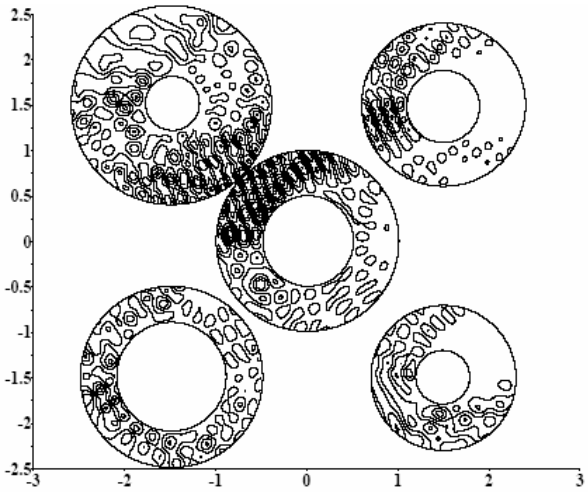

Fig. 10. Contour of the real-part solution.
(Helmholtz-exterior acoustics)

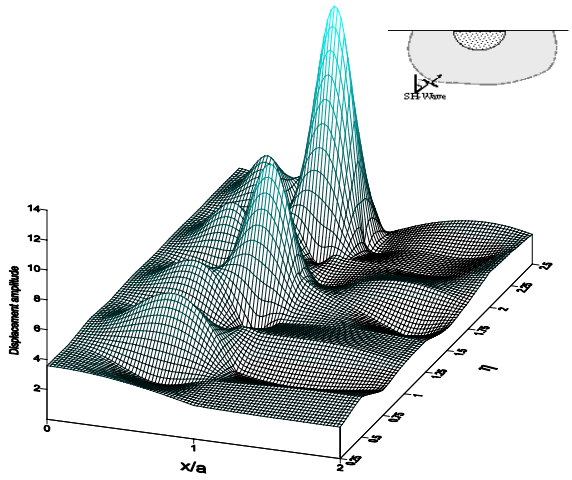

Fig.11. Surface displacements for the vertical incidence plotted versus the dimensionless frequency η.
(Helmhotlz equation-half plane problems)

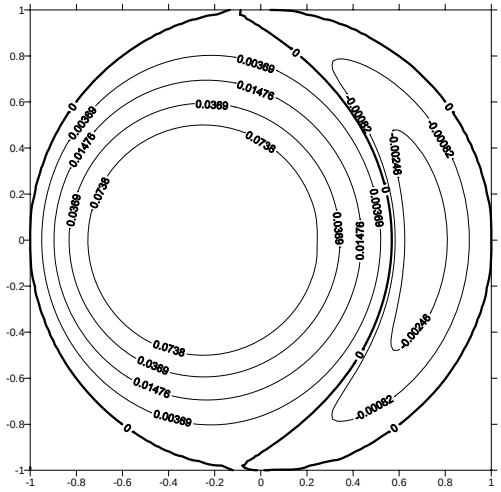

Fig. 12. Stream function of Stokes' problem.
(biharmonic equation)

ANECDOTES

I began my teaching job in NTOU since August, 1994. I remembered at that time that Prof. Hwang was the Dean of the College of Engineering and Science. He invited the new members of the College to enjoy a delicious lunch on the ship of NTOU-Ocean Researcher No.2. He supported the new staff for the equipment fee. He left NTOU in 1995. Eight years later in 2003, he returned NTOU to be the President. I was impressed that he always encouraged me as well as younger researchers to do a good job in teaching and research. Under the mechanism of encouragement in NTOU, I was promoted to be the Distinguished Professor in 2005 and won the Academic Achievement Award in 2006. Besides, it is a good memory for my families to swim in the pool with Prof. Hwang. He showed me his ambition in learning swimming even at the age over sixty. Finally, he can swim. I learned from him that no one is too old to learn and never give up. Hope that he will have a fruitful life after retirement.

A picture of President Hwang (in the center) and the author (in the right).

Fig.1. Sketch of null-field and domain points in conjunction with the adaptive observer system (left: boundary point, right: null-field point).
Fig.2. The degenerate kernel for one, two and three dimensional problems.
Fig.3. Stress around the hole of radius a_1. **(Laplace equation)**
Fig.4. Displacement for the circular bar weakened by three holes. **(Laplace equation)**
Fig.5. Contour of stress concentration for $D/d = 0.0625$. **(Laplace equation)**
Fig.6. Tangential stress distribution around the inclusion located at the origin. **(Laplace equation)**
Fig.7. Contour of shear stress $\sigma_{zy}/\tau_{\infty}$. **(Helmholtz equation)**
Fig.8. The first mode of eccentric membrane. **(Helmholtz equation)**
Fig.9. The first mode of eccentric plate. **(biHelmholtz equation)**
Fig.10. Contour of the real-part solution. **(Helmholtz-exterior acoustics)**
Fig.11. Surface displacements for the vertical incidence plotted versus the dimensionless frequency η. **(Helmhotlz equation-half plane problems)**
Fig.12. Stream function of Stokes' problem. **(biharmonic equation)**

Hwang-65.doc by Chen J T April, 20, 2006.